

35. DIORITIC BASEMENT, SITE 493: PETROLOGY, GEOCHEMISTRY, AND GEODYNAMICS¹

H. Bellon, Groupe de Recherche Géochronologique, Laboratoire de Pétrologie,
Université Paris-Sud, 91405 Orsay Cédex, France

R. C. Maury and J. F. Stephan, Université de Bretagne Occidentale, 29283 Brest Cédex, France,
and G.I.S. 9 Océanologie et Géodynamique, CNRS-UBO-CNEXO

ABSTRACT

At Site 493, DSDP Leg 66, dioritic basement was reached below lower Miocene (NN1 Zone, 22–24 Ma) terrigenous sediments. Petrographical, mineralogical (including microprobe analyses), and chemical features of the dioritic rocks reveal their magmatic affinity with the calc-alkaline series. Furthermore, their radiometric age (35.3 m.y.) links the basement to the Sierra Madre Occidental in Mexico and to mid-Tertiary volcanic arcs in Central America. The presence of Oligocene diorite 50 km from the trench axis confirms the truncation of the south Mexico margin, which we explain as the result of a 650 to 800 km left-lateral displacement of Central America relative to North America. Truncation must have occurred in the late Miocene, after the diorite intrusion and prior to the present subduction.

INTRODUCTION

In the course of Leg 66, a total of eight sites were drilled on a transect of the Middle America Trench, southeast of Acapulco, Mexico: a reference oceanic site on the Cocos Plate (487), one in the trench (486), four on the lower and middle slopes (489, 491, 492, 490), and two on the upper slope, with continental basement (489, 493) (Fig. 1). Site 489, 30 km from shore, bottomed in garnet-micaschists beneath approximately 300 meters of Pleistocene and lower Miocene terrigenous sediments. Site 493, 15 km from the coast, was drilled under 645 meters of water. The dioritic basement appeared under 650 meters of muddy silt and sands ranging from Pleistocene to lower Miocene with a hiatus in the middle Miocene. The lower Miocene sequence, very sandy at the base, is transgressive upon the dioritic body; the oldest dated levels correspond to the NN1 Zone—i.e., 22.24 Ma (Ryan et al., 1974).

We penetrated approximately 25 meters of dioritic basement (Cores 493-58, 493-59, and 493-60) and studied Samples 493-59-1, 42–63 cm and 62–67 cm; 493-59-2, 98–102 cm; and 493-60-1, 101–104 cm; for convenience, Sample 493-59-1, 62–67 cm will be labeled 493-59-1A hereafter.

ANALYTICAL RESULTS

Petrography

The four diorite samples (493-59-2, 493-59-1, 493-59-1A, and 493-60-1) have a coarse, granular structure. Large tabular plagioclase crystals are their major component. Alkali feldspar occurs as rare interstitial crystals of small size, often in association with quartz crystals that are also interstitial and not very abundant. The mafic minerals are represented by idiomorphic green

hornblende, often rich in ilmenite inclusions. Some hornblende crystals exhibit an optical zoning marked by more intense green zones. Biotite (often chloritized) occurs either as large idiomorphic crystals devoid of zircon inclusions or as smaller ones rimming amphiboles or even located within their cleavages. Ilmenite is the only primary oxide phase and occurs as individual crystals or as inclusions within mafic phases; it is sometimes altered to hematite. Accessory minerals include apatite (common), sphene and epidote (rare), and sericite developed at the expense of plagioclase.

In comparison with Samples 493-59-2, 493-59-1, and 493-60-1, Sample 493-59-1A is fine grained and rich in amphibole and biotite; imbricated plagioclase laths make it doleritic in aspect.

Mineralogy

Microprobe data (Tables 1–3) were obtained on the freshest diorite sample, 493-59-1A, using a Camebax automated microprobe (Microsonde Ouest, Brest), the working conditions of which are 15 kV, 10–12 nA; 6-s counting time; correction by (Z)(A)(F) method. Concentrations lower than 0.1% cannot be considered as representative in these conditions.

Hornblendes (Table 1; Fig. 2) range in composition from actinolitic hornblende to magnesiohornblende and ferrotschermakitic hornblende. The core (Fig. 2, Nos. 1, 2) and the extreme periphery (6, 7) of large crystals are usually made of actinolitic hornblende and the intermediate areas and smallest crystals, of magnesiohornblende (5, 9). The greenest zones have a very distinct composition, which plots into the ferrotschermakitic hornblende field (4, 8). The trend from actinolitic hornblende to ferrotschermakitic hornblende is characterized by important chemical variations involving an increase of Ti, Al, Fe, Mg, and Na and a corresponding decrease of Si and Mg, Ca remaining approximately constant.

Biotites have an iron-magnesium ratio close to 0.5 (Table 2, Analyses 10–13), and there are no noticeable

¹ Initial Reports of the Deep Sea Drilling Project, Volume 66.

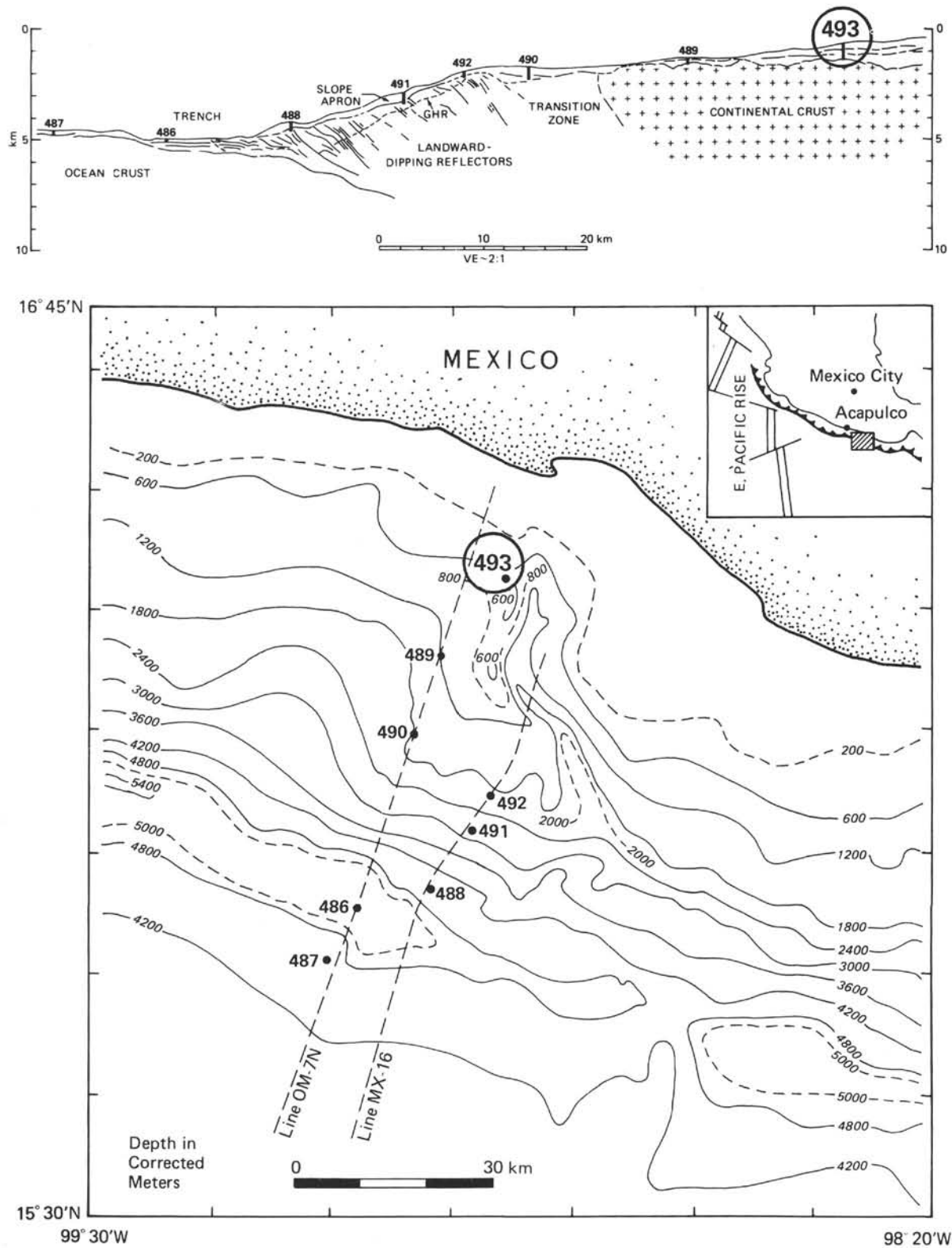


Figure 1. Geological and geographical setting of Site 493 (after Moore et al., 1979a, 1979b).

Table 1. Hornblende analyses (Sample 493-59 1A).

Analysis	1	2	3	4	5	6	7	8	9
SiO ₂	49.68	49.57	49.59	41.66	45.54	51.21	50.58	41.88	47.87
TiO ₂	0.75	0.74	1.00	2.60	1.68	0.68	0.53	2.67	0.82
Al ₂ O ₃	5.63	5.32	6.05	12.16	9.14	4.28	4.52	12.31	6.95
Cr ₂ O ₃	0.00	0.00	0.05	0.00	0.01	0.00	0.12	0.00	0.00
FeO*	15.78	15.65	15.63	18.16	16.49	14.26	14.39	18.56	16.25
MnO	0.42	0.58	0.27	0.44	0.42	0.49	0.34	0.32	0.34
MgO	12.59	13.01	12.69	8.51	10.44	13.73	13.63	8.31	11.93
CaO	11.93	12.11	12.09	11.97	11.88	12.00	11.37	11.92	12.24
Na ₂ O	0.65	0.60	0.71	1.47	1.17	0.49	0.38	1.48	0.82
K ₂ O	0.31	0.31	0.21	0.92	0.69	0.18	0.18	0.93	0.35
Total	97.74	97.89	98.29	97.89	97.46	97.32	96.04	98.38	97.57
Si	7.307	7.290	7.244	6.312	6.810	7.490	7.486	6.315	7.101
Ti	0.083	0.081	0.110	0.296	0.189	0.075	0.058	0.303	0.092
Al	0.976	0.922	1.041	2.171	1.612	0.737	0.788	2.187	1.214
Cr	0.000	0.000	0.005	0.000	0.001	0.000	0.014	0.000	0.000
Fe	1.941	1.924	1.910	2.301	2.062	1.744	1.781	2.340	2.016
Mn	0.052	0.073	0.033	0.056	0.053	0.060	0.042	0.041	0.043
Mg	2.761	2.853	2.764	1.921	2.327	2.992	3.008	1.867	2.638
Ca	1.880	1.909	1.893	1.943	1.903	1.880	1.803	1.926	1.945
Na	0.184	0.172	0.201	0.431	0.339	0.140	0.109	0.434	0.236
K	0.058	0.058	0.039	0.177	0.131	0.034	0.035	0.179	0.066
FM	0.419	0.412	0.413	0.551	0.476	0.376	0.378	0.560	0.438

Note: Structural formulae are based on 23 oxygens. FeO* is total iron expressed as FeO; FM = Fe + Mn/Fe + Mn + Mg. 1-7 = core-to-rim compositions of a crystal 250 μ m in diameter. (1 = core; 7 = rim; 20 μ m between two successive points). Point 4 corresponds to a green zone, Point 5 to a light green one. 8 = analysis of a green zone from a crystal 200 μ m in diameter. 9 = analysis of the core of a small crystal (20 μ m in diameter).

compositional variations from large crystals to smaller ones petrographically linked to amphiboles.

Ilmenite also has a very constant composition (Table 2, Analyses 14-16), characterized by a low percentage (~2.5%) of hematite in solid solution and a low amount of MgO; the MnO content increases with decreasing size of the crystals.

Feldspars (Table 3). Plagioclase (Analyses 17-22) ranges in composition from labradorite to oligoclase. Zoning is predominantly normal (though sometimes oscillatory), the most sodic composition corresponding to the small crystals and to the peripheries of the larger ones. Alkali feldspar occurs quite rarely as small interstitial crystals of nearly pure orthoclase composition (23, 24).

Incidence for K-Ar dating. Potassium appears to be concentrated mainly in the biotites (10% K₂O) and much more accessorially into the rare interstitial orthoclase crystals. The K₂O contents of amphibole and plagioclase remain lower than 1% and 0.2%, respectively.

Chemistry

Two chemical analyses (Table 4) give some idea about the range of major oxides in the dioritic pluton: SiO₂ ~54.4% (the rocks contain a little normative quartz), Al₂O₃ ~16.7%. In the two rocks, the weight percentages of CaO and (Na₂O + K₂O) are equal: 6.03-5.74 and 6.26-5.84. But there is a large variation in the alkaline elements Na₂O and K₂O; in one rock, the K₂O/Na₂O ratio is equal to 0.88, in the other, it is 0.42. In the AFM diagram (Fig. 3), the two rocks are located in the area of the low Si calc-alkaline tertiary lavas from Central America (McBirney, 1969).

Radiometric K-Ar Analyses

We calculate three model ages using the following age circulation formula based on the decay constants and isotopic ratios compiled by Steiger and Jäger (1977): $T_{(m.y.)} = 4153.9 \log_{10} [1 + 142.33 (40 \text{ Ar}^{*2}/\text{K})]$. K contents in grams are determined by atomic absorption on two independent wet chemical attacks (HF + HClO₄ + H₂SO₄), and radiogenic argon (40 Ar*) content is measured by mass spectrometry using the isotopic technique.

Whole-rock samples crushed into fragments (0.15-0.75 mm in size) are boiled in a molybdenum crucible heated by induction currents. The spike (38 Ar) is buried as positive ions, by a 30-keV source, into an aluminum foil target 1 sq. cm in area (Bellon et al., in press). This target is added to the sample at time t_0 (weighing time) of the experiment and is thus fused with the rock. Active

²* = radiogenic argon.

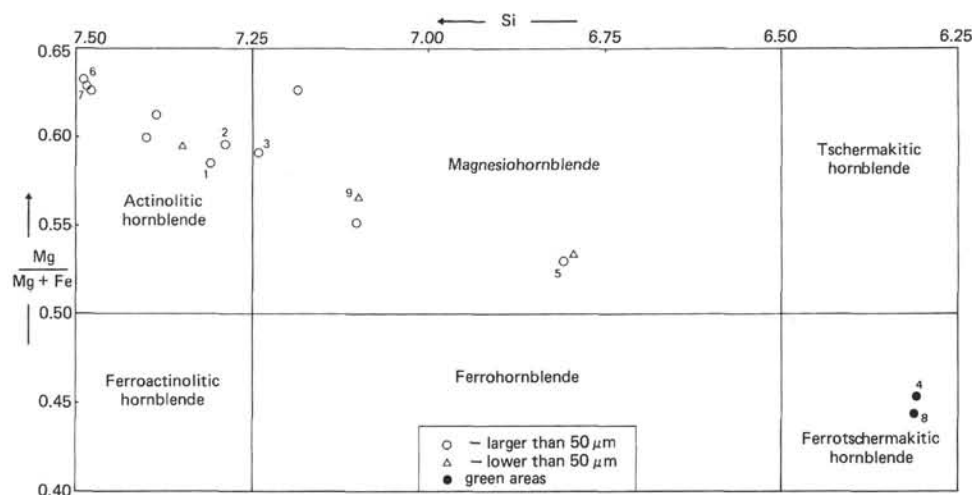


Figure 2. Position of the amphiboles in Sample 493-59-1A. (After Leake's 1978 classification diagram of calcic amphiboles; Si coordinates are numbers of atoms of the standard formula based on 23 oxygens; 1-9 correspond to the analyses in Table 1; 1-7 are core-to-rim zoning of a single crystal 250 μ m in diameter.)

Table 2. Biotite and ilmenite analyses (Sample 493-59 1-A).

Analysis	Biotite				Ilmenite			
	10	11	12	13	σ	14	15	16
SiO ₂	36.56	35.42	36.74	36.41	0.60	0.00	0.00	0.00
TiO ₂	3.07	3.29	3.11	3.35	0.21	51.58	51.73	51.50
Al ₂ O ₃	15.10	14.71	15.08	14.83	0.25	0.00	0.00	0.00
Cr ₂ O ₃	0.07	0.09	0.00	0.04	0.04	0.04	0.00	0.04
Fe ₂ O ₃						2.78	2.59	2.50
FeO	19.12*	20.01*	19.43	19.76*	0.54	44.37	44.61	43.87
MnO	0.24	0.10	0.24	0.17	0.08	1.73	1.88	2.40
MgO	11.60	11.36	11.10	11.41	0.30	0.16	0.00	0.01
CaO	0.00	0.01	0.14	0.02	0.04	0.00	0.00	0.05
Na ₂ O	0.04	0.16	0.13	0.14	0.04	0.01	0.00	0.00
K ₂ O	10.54	10.28	10.13	10.24	0.18	0.00	0.03	0.02
Total	96.34	95.43	96.10	96.37		100.67	100.84	100.39
FM	0.484	0.498	0.498	0.495				

Note: Total iron expressed as FeO (*) for biotites and distributed between Fe₂O₃ and FeO following Carmichael's (1967) method for ilmenites. 10 and 11 = core and rim of a biotite crystal 100 μ m in diameter. 12 = small biotite crystal (20 μ m) associated to amphibole. 13 = mean analysis (σ = standard deviation) of biotites from Sample 493-59-1A (10 analyses). 14, 15, 16 = cores of ilmenite crystals 200 μ m, 100 μ m, and 50 μ m, respectively, in size.

Table 3. Feldspar analyses (Sample 493-59-1A).

Analysis	17	18	19	20	21	22	23	24
SiO ₂	52.70	54.63	60.52	59.14	57.31	61.11	61.84	64.35
Al ₂ O ₃	29.65	28.28	24.61	24.68	27.04	24.20	18.63	18.83
Fe ₂ O ₃	0.00	0.01	0.01	0.07	0.21	0.06	0.11	0.09
MnO	0.09	0.01	0.00	0.00	0.00	0.00	0.00	0.11
CaO	12.20	10.83	6.55	6.89	9.30	5.75	0.05	0.00
Na ₂ O	4.99	5.92	8.81	8.34	6.74	8.41	0.34	0.18
K ₂ O	0.08	0.11	0.18	0.13	0.12	0.24	17.30	18.34
Total	99.71	99.79	100.68	99.25	100.72	99.77	98.27	101.90
Ca	57.2	50.0	28.8	31.1	43.0	27.1	0.2	0.0
Na	42.3	49.4	70.3	68.2	56.4	71.6	2.9	1.5
K	0.5	0.6	0.9	0.7	0.7	1.3	96.9	98.6

Note: Total iron expressed as Fe₂O₃; TiO₂ and MgO contents have been found equal to zero in all the cases. 17-20 = core-to-rim composition of a crystal 150 μ m in diameter. 21 = core of a crystal 200 μ m in size. 22 = crystal 30 μ m in size. 23 and 24 = potassic feldspars, less than 20 μ m in diameter.

gases are eliminated by four titanium sponge furnaces and a titanium-zirconium getter before isotopic analysis in a 180° stainless steel mass spectrometer. The weak mass discrimination is corrected after each measurement with air argon standards proportionate to the volume of argon in the sample.

The resulting radiometric data (Table 5) correlate well and indicate an age of 35.5 ± 1.7 m.y. for the dioritic pluton. The slight discrepancy among results may relate to the K₂O contents of the samples—i.e., the maximum mean age may correspond to the lowest K₂O value and the minimum mean age to the highest value.

DISCUSSION

Correlation with Magmatic Episodes in Mexico

South Coast

On land, near Leg 66 sites (between Acapulco and Puerto Angel, Fig. 4), most outcrops correspond to pre-Mesozoic basement intruded by numerous plutons of various ages (cf. synthesis and references in Butterlin, 1977, and in Tardy, 1980). Some of these intrusives—for example, the plutons of the Acapulco area (Acapulco granite and El Ocotito and Xaltianguis quartz-monzonite), which reveal a complex magmatic his-

Table 4. Major oxides in the dioritic pluton.

	Sample 493-59-1, 62-67 cm	Sample 493-59-1, 42-63 cm
Chemical Analyses		
SiO ₂	55.81	53.25
TiO ₂	1.40	1.33
Al ₂ O ₃	15.83	16.64
Fe ₂ O ₃	1.50	1.50
FeO	6.22	6.47
MnO	0.06	0.07
MgO	3.81	4.92
CaO	6.27	6.03
Na ₂ O	4.14	3.05
K ₂ O	1.70	2.69
P ₂ O ₅	0.40	0.33
H ₂ O +	2.54	3.22
H ₂ O -	0.19	0.16
CO ₂	0.0	0.0
Total	99.87	99.66
CIPW Norm		
Qz	5.71	2.98
Or	10.34	16.51
Ab	36.05	26.79
An	20.17	24.69
*Wo	3.82	1.73
*En	2.01	0.97
*Fs	1.69	0.68
En	7.75	11.75
Fs	6.52	8.22
Emt	2.24	2.26
Il	2.74	2.62
Ap	0.98	0.81
SUMD	100.02	100.02

Note: Analysts are R. Duret and A. Pantaloni, Laboratory of Petrology, University of Paris-Sud, Orsay. SiO₂, Al₂O₃, TiO₂, total iron, CaO, and MgO are determined by X-ray fluorescence on a glassy pearl; K₂O and Na₂O, by atomic absorption; and FeO, by complexometry.

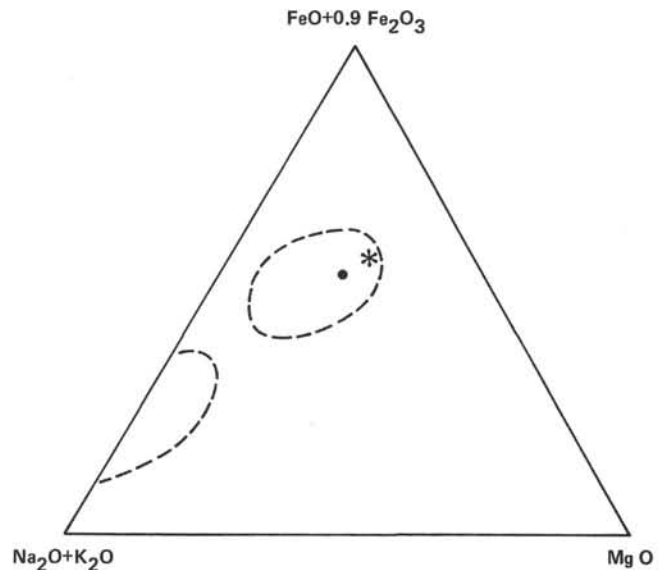


Figure 3. Position of Site 493 dioritic samples in AFM diagram. (● = Sample 493-59-1, 62-67 cm; * = Sample 493-59-1, 42-63 cm; --- = Tertiary calc-alkaline lavas from Central America [McBirney, 1969].)

Table 5. Radiometric K-Ar analyses.

Sample (interval in cm)	Mean Value (\pm uncertainty)	Calculated Model Age	Radiogenic $^{40}\text{Ar}^*$ (10^{-6} cc/g)	(%) $\frac{^{40}\text{Ar}^*}{^{40}\text{Ar}_T}$	Fused Weight	K_2O	Experiment No.
493-59-2, 98-102	35 ± 2	33	2.685	57.1	1.0001	2.48	3127 C/2
		37	3.012	61	1.0122	2.48	3070 C/2
493-59-1, 62-67	36.4 ± 1.8	35.1	2.13	60.3	1.0014	1.85	3043 B/1
		37.7	2.29	63.6	1.0262	1.85	3042 B/1
493-59-1, 42-63	34.5 ± 2	35.6	3.05	65.6	1.0251	2.61	3069 C/2
		33.3	2.85	54	1.0053	2.61	3125 D/4

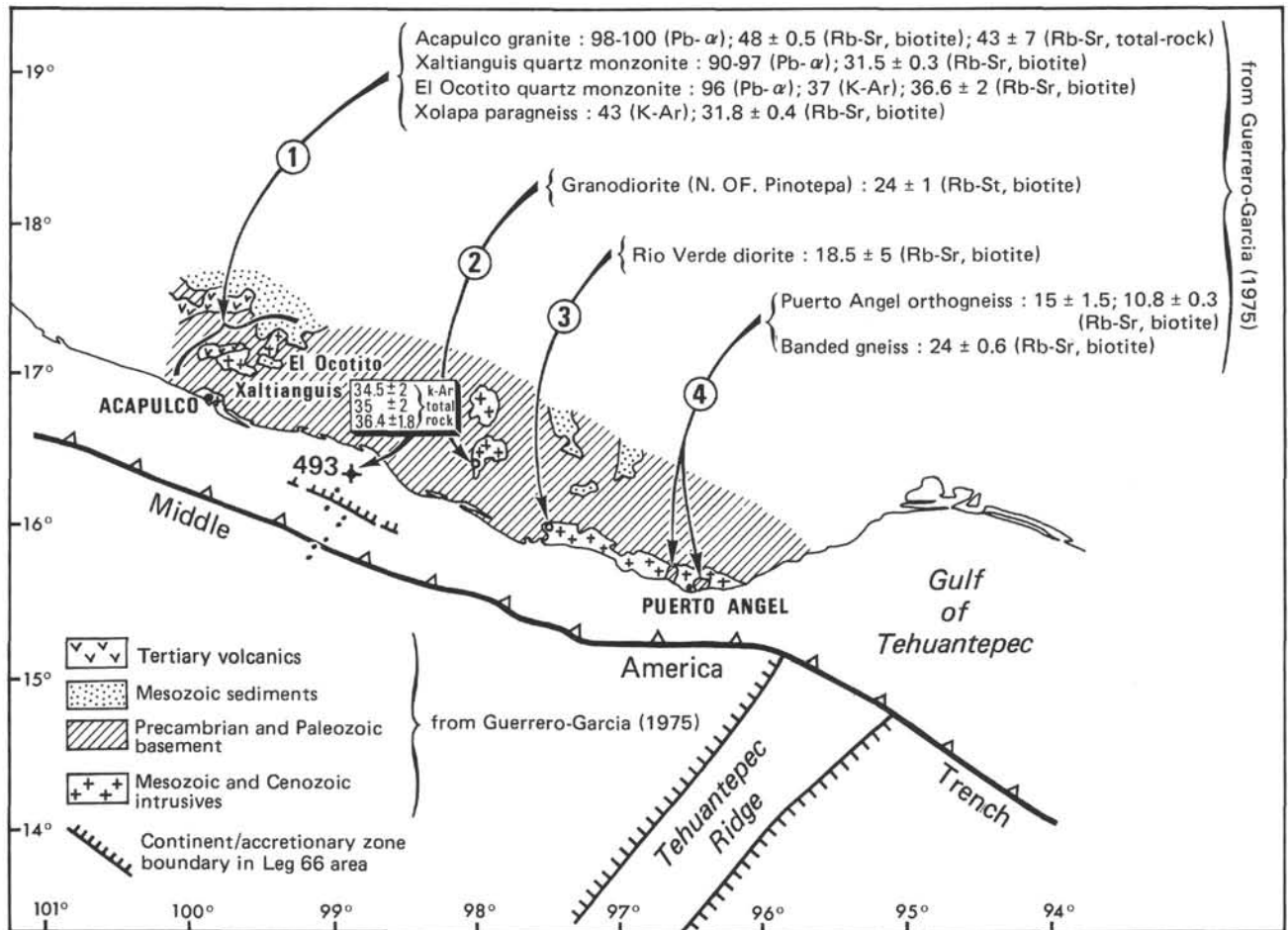


Figure 4. Isotopic ages from land outcrops in Leg 66 area (states of Guerrero and Oaxaca, southern Mexico).

tory—are Mesozoic and Cenozoic. In effect, the radiometric data on these intrusions, obtained by various methods, indicate three age groups (Guerrero, 1975³): Middle Cretaceous (90–100 Ma, Pb- α); Eocene (43–48 Ma, K-Ar and Rb-Sr); and Oligocene (31–36 Ma, Rb-Sr). The first age group is obtained only by applying the Pb- α method. Moreover, although Guerrero (1975) believes the intrusion of the Acapulco granite occurred 48 Ma, if the 90–100 Ma date is significant 48 Ma dates remobilization, not original intrusion.

However that may be, the interesting fact is the existence of a 31–36 Ma age group for the intrusives as well as for the Paleozoic/Precambrian paragneiss. This

implies a thermal rise sufficient to rejuvenate the old basement by a complete opening up of the system, as suggested by Guerrero (1975). Thus it appears that the mean age obtained for the various samples in dioritic basement at Site 493 assigns them to the 31–36 Ma family in the Acapulco area and probably includes not only true Oligocene intrusions but also older intrusions reactivated by the thermal event. It must nevertheless be noted that ages more recent than 35 Ma and decreasing progressively from west to east (24–10.8 Ma) have been ascertained for granodiorites and gneiss in the area between Acapulco and Puerto Angel (Fig. 4, from Guerrero, 1975). One must therefore admit that (tectonic and/or thermal?) post-Oligocene events affected this area close to the Tehuantepec Gulf.

³ The ages Rb-Sr alone are from this author; the others are from earlier studies.

Northern Mexico

North of the Trans-Mexican Volcanic Belt (Plio-Quaternary, < 5 Ma, Gastil et al., 1979), Mesozoic and Cenozoic magmatism outcrop over a very large area. They have been the subject of a number of detailed petrological, geochemical, and geochronological studies.

If we consider Tertiary volcanism alone, two large masses are apparent (Fig. 5). One centers around the Gulf of California and is developed mainly on the eastern side of the Baja California Peninsula. It corresponds to various magmatic episodes ranging from early Miocene up to Recent (post-22 Ma, after Gastil et al., 1979). The backbone of the second is in the Sierra Madre Occidental; McDowell and Clabaugh (1979) identified two main calc-alkaline magmatic episodes: the first, uninterrupted, from 100 to 45 Ma, the second appearing after 10 m.y. of apparent magmatic quiescence and corresponding to the ignimbritic "explosion," which began 35 Ma. This activity, which continued for 7 m.y., reached its peak between 30 and 28 Ma (McDowell and Clabaugh, 1979).

Northeast of the Sierra Madre Occidental and in continuous outcrop with it, these authors recognized two other provinces (Fig. 5): Eastern Chihuahua, with intermediate suites (calc-alkaline-alkaline) and a peak of activity between 32 and 30 Ma, and Trans-Pecos Texas, typically alkaline, with a peak of activity 36 to 34 Ma.

It must be noted (McDowell and Clabaugh, 1979) that if the second magmatic episode is relatively short in the Sierra Madre Occidental (34–22 Ma), activity occurs over a wide range of time (from 50–16 Ma) in Trans-Pecos Texas.

Bearing in mind all these data, we can conclude (1) that the diorite at Site 493 and intrusives the same age or younger in the Acapulco area are clearly located in the prolongation of the Sierra Madre Occidental (Fig. 5) and (2) its calc-alkaline composition as well as its age (35.3 m.y.) make it possible to locate the diorite in the second magmatic episode (35–28 Ma) of the Sierra Madre Occidental.

Consequences of the Evolution of the South Mexico Active Margin

Above all, and to remain as objective as possible, we propose to work on two hypotheses.

1) Although we will consider, as is generally admitted, that calc-alkaline magmatism is a tracer of subduction, one must remember that a dephasing of some million years may have taken place between the initiation of subduction and its magmatic surface expression.

2) We will admit that although (calc-alkaline) volcanism and plutonism have the same significance and the same relationship with global geodynamic processes, the mechanism of magma ascension to the surface (volcanism) or to the subsurface (plutonism and hypovolcanism) reflects different conditions of stress in the basement.

According to these hypotheses, the diorite at Site 493 and the intrusives of the Acapulco area belong to an Oligocene arc, a southern extension of the Sierra Madre

Occidental arc. The latter is usually considered to be the expression of the eastward-bound subduction (beneath the North American continent) of the Farallon Plate (Atwater, 1970; Demant and Robin, 1975). One must remember, however, that the period of activity of this arc was relatively brief (about 7 m.y.) and that the nature of its volcanism is in some respects original (McDowell and Clabaugh, 1979).

Nevertheless, the presence of an Oligocene arc approximately 50 km from the present Middle America Trench can be understood only if one considers the margin to be truncated. Indeed, if we take into account the near and active example of the Central America volcanic arc, at least 150 km from the trench axis, there is a minimum of 100 km of continent and/or accretionary zone, facing the coast of southern Mexico, missing from the Oligocene structure.

The idea of continental margin truncation in this area is not new (Karig et al., 1978, including references). For example, the absence of belts of subduction complexes such as exist in Baja California and Central America, the existence of Cretaceous plutons of the Acapulco type along the coast, and the fact that the structural trends in the pre-Mesozoic basement are truncated at a right angle by the present trench have been used in support of the idea. Likewise, the Middle to Upper Cretaceous overthrusts are intersected by the present coast between Acapulco and the Gulf of Tehuantepec (Tardy, 1980; Cordoba et al., 1980).

If we use the Oligocene arc as a guide, we must search for its equivalent and that of its extension toward the southeast. This equivalent exists in Central America immediately south of the left-lateral strike-slip fault system of Polochic-Motagua. The first well-documented (Sutter, 1977) Cenozoic volcanic episode is Oligocene (30–25 Ma). It is more or less parallel to the recent volcanic Plio-Quaternary arc (cf. map by Case and Holcombe, 1980, and Fig. 5).

To re-establish the continuity of this Oligocene arc by making use of the transform system of Polochic-Motagua, a right-lateral displacement of 650 to 800 km must have occurred. This distance is only approximate, since (1) doubt remains concerning the exact position of the Oligocene arc on either side of the Polochic-Motagua transform zone and (2) we posit a volcanic arc that originally had a regular trend—i.e., without contorsion or break.

As for the age of this left-lateral displacement, it is necessarily posterior to the intrusion of the diorite at Site 493—i.e., to 35 Ma—and earlier than the oldest accreted turbidites at Site 492—i.e., before the pre-late Miocene. The top limit is confirmed by the fact that the volcanism of the Trans-Mexican Axis, which is generally considered to be linked to the present subduction of the Cocos Plate under the south Mexico margin (Demant, 1978), began with the Pliocene (Gastil et al., 1979).

CONCLUSION

The Oligocene (35.3 Ma) diorite at Site 493 is located in the exact prolongation of the volcanic arc of the same

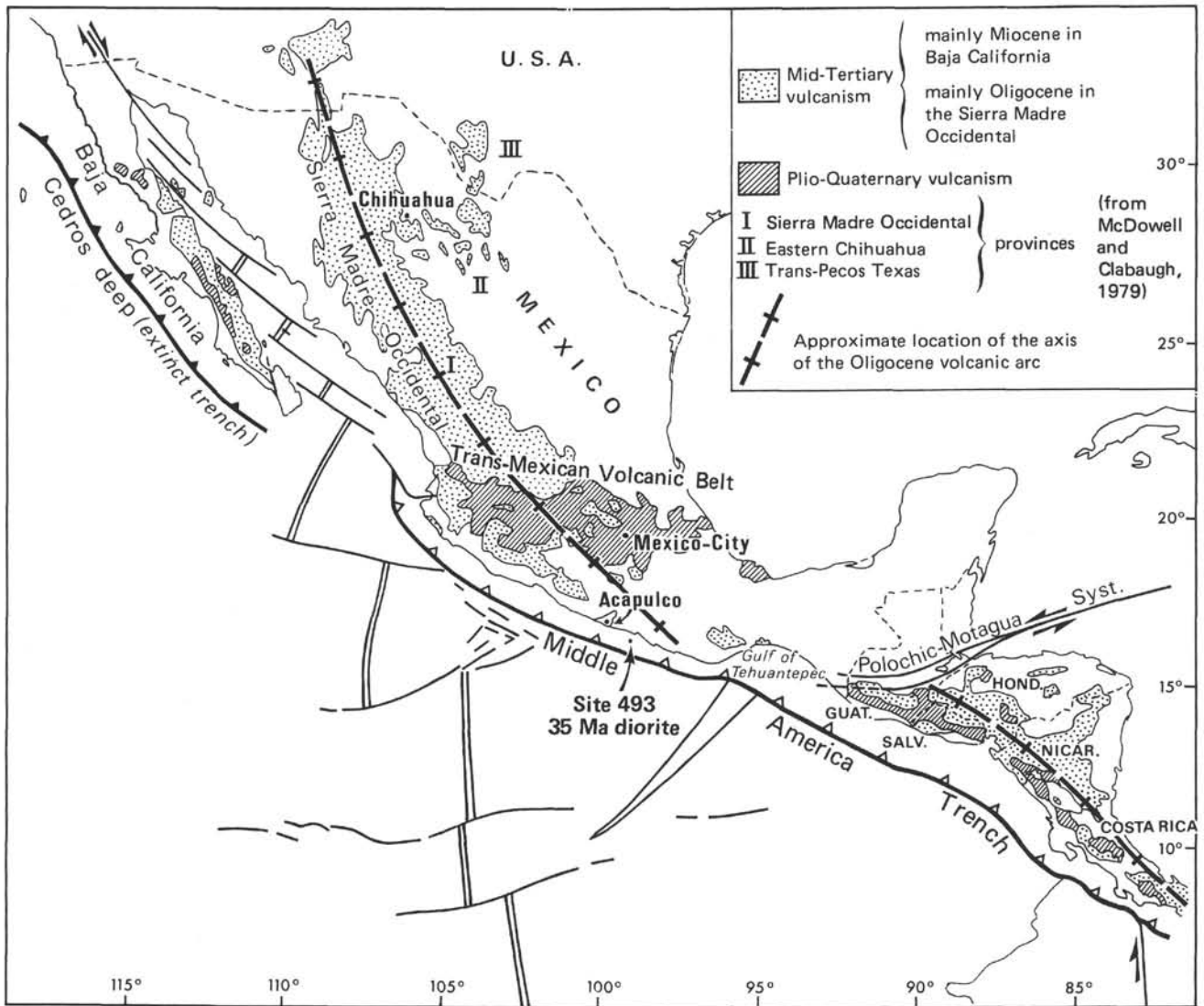


Figure 5. Cenozoic magmatic belts in Mexico and northern Central America.

age represented by NW-SE Sierra Madre Occidental north of the E-W Plio-Quaternary Trans-Mexican Volcanic Belt. That it is less than 30 km from the oldest known accreted turbidites, at the top of the accretionary zone, suggests a major truncation of the south Mexico margin at that level. This truncation may, for example, be the result of eastward displacement of Central America along a system of pre-Polochic-Motagua strike-slip faults. Taking into account various constraints, this left-lateral displacement, of about 650 to 800 km, took place during the Miocene.

ACKNOWLEDGMENTS

The present study was achieved within the framework and with the financial support of the A.T.P. IPOD of the CNRS (contract 42-32). We wish to thank R. Duret, J. C. Philippet, and A. Pantaloni for their technical assistance and C. Rangin and M. Tardy for their share of very fruitful discussions.

REFERENCES

- Atwater, T., 1970. Implications of plate tectonic for the Cenozoic tectonic evolution of Western North America. *Geol. Soc. Am. Bull.*, 81:3513-3536.
- Bellon, H., Buu, N., Chaumont, J., et al., in press. Implantation ionique d'argon dans une cible support. Application au tracage isotopique de l'argon contenu dans les minéraux et les roches. *C. R. Acad. Sci., Paris*.
- Butterlin, J., 1977. *Geologie structurale de la région des Caraïbes, Mexique, Amérique centrale, Antilles et Cordillère caraïbe*: Paris (Masson).
- Carmichael, I. S. E., 1967. The iron-titanium oxides of salic volcanic rocks and their associated ferromagnesian silicates. *Contrib. Mineral. Petrol.*, 14:36-64.
- Case, J. E., and Holcombe, T. L., 1980. *Geological-tectonic map of the Caribbean region*: Reston, Va. (U.S. Geological Survey).
- Cordoba, D. A., Tardy, M., Carfantan, J. C., et al., 1980. Le Mexique mésogéen et le passage au système cordillérain de type Californie. *26ème Congr. Géol. Int.*, Paris, Colloque C5:18-29.
- Demant, A., 1978. Características del Eje Neovolcanico Transmexicano y sus problemas de interpretación. *Rev. Inst. Geol. UNAM*, 2 (2):172-187.
- Demant, A., and Robin, C., 1975. Las fases de vulcanismo en México: una síntesis en relación con la evolución geodinámica desde el Cretácico. *Rev. Inst. Geol. UNAM*, 1(1):70-83.
- Gastil, G., Krummenacher, D., and Minch, J., 1979. The records of Cenozoic volcanism around the Gulf of California. *Geol. Soc. Am. Bull.*, 90:839-857.
- Guerrero-García, J. C., 1975. Contributions to paleomagnetism and Rb-Sr geochronology [Ph.D. dissert.]. University of Texas, Dallas.

- Karig, D. E., Cardwell, R. K., Moore, G. F., et al., 1978. Late Cenozoic subduction and continental margin truncation along the Northern Middle America Trench. *Geol. Soc. Am. Bull.*, 89: 265-276.
- Leake, B. E., 1978. Nomenclature of amphiboles. *Bull. Mineral.*, 101:453-467.
- McBirney, A. R., 1969. Compositional variations in Cenozoic calc-alkaline suites of Central America. *Proc. Andesite Conf., Int. Upper Mantle Project Sci. Rept.*, 16, State of Oregon:185-189.
- McDowell, F. W., and Clabaugh, S. E., 1979. Ignimbrites of the Sierra Madre Occidental and their relation to the tectonic history of western Mexico. *Geol. Soc. Am. Spec. Pap.*, 180:113-124.
- Moore, J. C., Watkins, J. S., Bachman, S. B., et al., 1979a. Off Mexico Middle America Trench. *Geotimes*, 24:20-22.
- _____, 1979b. Progressive accretion in the Middle America Trench, Southern Mexico. *Nature*, 281:638-642.
- Ryan, W. B. F., Cita, M. B., Dreyfus, R. M., et al., 1974. A paleomagnetic assignment of Neogene stage boundaries and the development of isochronous datum planes between the Mediterranean, the Pacific and Indian oceans, in order to investigate the response of the World Ocean to the Mediterranean "salinity crisis." *Riv. Ital. Paleont.*, 80:631-688.
- Steiger, R. H., and Jäger, E., 1977. Sub-commission on geochronology: Convention on the use of decay constants in geo- and cosmochronology. *Earth Planet. Sci. Lett.*, 26:359-362.
- Sutter, J. F., 1977. K/Ar ages of Cenozoic volcanic rocks in Northern Central America. *8th Caribbean Geol. Conf. Abstr.*, Curacao. (Abstract)
- Tardy, M., 1980. Contribution à l'étude géologique de la Sierra Madre Orientale du Mexique [Ph.D. dissert.]. Université Pierre et Marie Curie, Paris.